Research Article
Viral Hepatitis

JOURNAL
OF HEPATOLOGY

TLR9 signalling in HCV-associated atypical memory B cells triggers Th1 and rheumatoid factor autoantibody responses

Graphical abstract

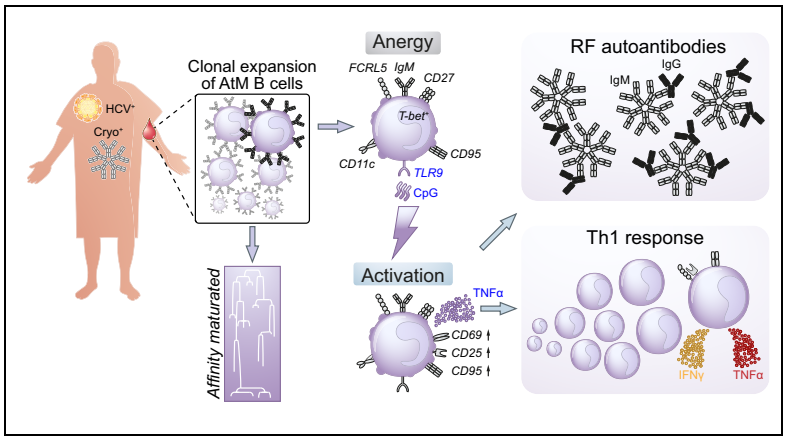

Highlights

- TLR9 activation of atypical memory B cells (AtMs) has a central role in breaking tolerance in patients with HCV-CV.
- TLR9 signaling on AtMs stimulates proliferation and activation of effector Th1 cells by secreting TNFα.
- Rheumatoid factors produced by AtMs recognized distinct IgG-Fc epitopes and did not cross-react against HCV proteins.
- AtMs largely disappear after antigen removal by DAA therapy.

Authors

Cloé Comarmond, Valérie Lorin, Cindy Marques, ..., Patrice Cacoub, Hugo Mouquet, David Saadoun

Correspondence

hugo.mouquet@pasteur.fr
(H. Mouquet) david.saadoun@aphp.fr
(D. Saadoun)

Lay summary

B cells are best known for their capacity to produce antibodies, which often play a deleterious role in the development of autoimmune diseases. During chronic hepatitis C, deleterious B cells proliferate and can be responsible for autoimmune symptoms (arthritis, purpura, neuropathy, renal disease) and/or lymphoma. Direct-acting antiviral therapy clears the hepatitis C virus and eliminates deleterious B cells.

http://dx.doi.org/10.1016/j.jhep.2019.06.029
 J. Hepatol. 2019, 71, 908–919

Research Article
Viral Hepatitis

JOURNAL OF HEPATOLOGY

TLR9 signalling in HCV-associated atypical memory B cells triggers Th1 and rheumatoid factor autoantibody responses

Cloé Comarmond[1,2,3,4,5,†], Valérie Lorin[4,5,†], Cindy Marques[3,4,5,†], Anna Maciejewski-Duval[1,2,3], Nizar Joher[4,5], Cyril Planchais[4,5], Maxime Touzot[6,7,8], Lucie Biard[9,10], Thierry Hieu[4,5], Valentin Quiniou[1,2], Anne-Claire Desbois[1,2,3], Michelle Rosenzwajg[1,2], David Klatzmann[1,2,3], Patrice Cacoub[1,2,3], Hugo Mouquet[4,5,*,‡], David Saadoun[1,2,3,*,‡]

[1]*Sorbonne Université, INSERM UMR_S 959, Immunologie-Immunopathologie-Immunotherapie, i3 and Département Hospitalo-Universitaire Inflammation-Immunopathologie-Biotherapie, i2B, F-75651 Paris, France;* [2]*AP-HP, Groupe Hospitalier Pitié-Salpêtrière, Service de Biothérapie, F-75013 Paris, France;* [3]*AP-HP, Groupe Hospitalier Pitié-Salpêtrière, Département de Médecine Interne et Immunologie Clinique, F-75013 Paris, France;* [4]*Laboratory of Humoral Immunology, Department of Immunology, Institut Pasteur, Paris, France;* [5]*INSERM U1222, Paris, France;* [6]*INSERM U932, 26 rue d'Ulm, 75005 Paris, France;* [7]*Institut Curie, Section Recherche, 26 rue d'Ulm, 75005 Paris, France;* [8]*Laboratoire d'Immunologie Clinique, Institut Curie, 26 rue d'Ulm, 75005 Paris, France;* [9]*AP-HP, SBIM, Hôpital Saint-Louis, Université Paris Diderot, Paris 7, Paris, France;* [10]*INSERM, ECSTRA Team, CRESS UMR-S 1153, 75010 Paris, France*

Background & Aims: Hepatitis C virus (HCV) infection contributes to the development of autoimmune disorders such as cryoglobulinaemia vasculitis (CV). However, it remains unclear why only some individuals with HCV develop HCV-associated CV (HCV-CV). HCV-CV is characterized by the expansion of anergic $CD19^+CD27^+CD21^{low/-}$ atypical memory B cells (AtMs). Herein, we report the mechanisms by which AtMs participate in HCV-associated autoimmunity.

Methods: The phenotype and function of peripheral AtMs were studied by multicolour flow cytometry and co-culture assays with effector T cells and regulatory T cells in 20 patients with HCV-CV, 10 chronically HCV-infected patients without CV and 8 healthy donors. We performed gene expression profile analysis of AtMs stimulated or not by TLR9. Immunoglobulin gene repertoire and antibody reactivity profiles of AtM-expressing IgM antibodies were analysed following single B cell FACS sorting and expression-cloning of monoclonal antibodies.

Results: The $Tbet^+CD11c^+CD27^+CD21^-$ AtM population is expanded in patients with HCV-CV compared to HCV controls without CV. TLR9 activation of AtMs induces a specific transcriptional signature centred on TNFα overexpression, and an enhanced secretion of TNFα and rheumatoid factor-type IgMs in patients with HCV-CV. AtMs stimulated through TLR9 promote type 1 effector T cell activation and reduce the proliferation of $CD4^+CD25^{hi}CD127^{-/low}FoxP3^+$ regulatory T cells. AtM expansions display intraclonal diversity with immunoglobulin features of antigen-driven maturation. AtM-derived IgM monoclonal antibodies do not react against ubiquitous autoantigens or HCV antigens including NS3 and E2 proteins. Rather, AtM-derived antibodies possess rheumatoid factor activity and target unique epitopes on the human IgG-Fc region.

Conclusion: Our data strongly suggest a central role for TLR9 activation of AtMs in driving HCV-CV autoimmunity through rheumatoid factor production and type 1 T cell responses.

Lay summary: B cells are best known for their capacity to produce antibodies, which often play a deleterious role in the development of autoimmune diseases. During chronic hepatitis C, self-reactive B cells proliferate and can be responsible for autoimmune symptoms (arthritis, purpura, neuropathy, renal disease) and/or lymphoma. Direct-acting antiviral therapy clears the hepatitis C virus and eliminates deleterious B cells.

Introduction

Chronic HCV infection is associated with extrahepatic complications that are largely immunologically driven. Among those, cryoglobulinaemia and its clinical sequelae hold the strongest association. Cryoglobulins are readily detectable in 40–60% of HCV-infected patients,[1–3] whereas cryoglobulinaemia vasculitis (CV) develops in only 5–10% of the cases.[4,5] The presence of autoantibodies and T cells in vascular infiltrates as well as the observation that specific HLA alleles confer susceptibility to CV in HCV-infected patients support the autoimmune nature of this virus-associated pathology.[6,7] CV pathophysiology depends on the interaction between HCV and lymphocytes that directly modulate B- and T cell function, which ultimately leads to the polyclonal activation and expansion of B cells producing rheumatoid factors (RFs).[1,8] We previously reported abnormal immune responses mediated by T cells in patients with HCV-associated cryoglobulinaemia vasculitis (HCV-CV), with a quantitative defect in regulatory T cells (Tregs),[6] and a Th1 polarization.[9,10] HCV infection has been associated with

Keywords: Hepatitis C virus; Cryoglobulinemia vasculitis; Atypical memory B cells; Immunology, direct-acting antiviral.
Received 30 October 2018; received in revised form 24 June 2019; accepted 27 June 2019; available online 4 July 2019

* Corresponding authors. Addresses: Laboratory of Humoral Response to Pathogens, Institut Pasteur, 28 rue du Docteur Roux, 75015 Paris, France; Tel.: +33 (0) 140613612, fax +33 (0)1 44389165 (H. Mouquet), or Département de Médecine Interne et d'Immunologie Clinique, INSERM, UMR_S 959, Hôpital Pitié-Salpêtrière, 83 boulevard de l'hôpital, 75013 Paris; Tel.: +33 (0)142178009, fax: +33 (0)142178033 (D. Saadoun).
E-mail addresses: hugo.mouquet@pasteur.fr (H. Mouquet), david.saadoun@aphp.fr (D. Saadoun).
† The authors contributed equally to this work as co-first authors.
‡ The authors contributed equally to this work as co-senior authors.

lymphoproliferations, which likely result from an indirect process following the chronic antigenic stimulation of a limited pool of pre-existing autoreactive B cells. It has been proposed that persistently high levels of HCV-containing immune complexes stimulate the proliferation of RF-bearing B cells, but the precise antigen(s) and stimulatory mechanisms have remained elusive. Our group and others previously identified a clonal expansion of $CD27^+IgM^+CD21^{low/-}$ memory B cells, referred to as activated or atypical memory B cells (AtMs), in HCV-CV.[11,12] AtMs are clonal or clonally related, and mainly express the V_H1-69 IgH gene, which is also highly prevalent in HCV-associated lymphoproliferations.[11–13] These clonal cells express reduced levels of the complement receptor 2, CD21, which mirrors an anergic state.[14,15] AtMs are prone to undergoing apoptosis.[11,13] They do not proliferate upon BCR stimulation but respond to the TLR9 agonist CpG by expressing activator and proliferative markers.[11,13] Anergy is a well-known regulatory mechanism for maintaining immune tolerance of autoreactive cells.[14,15] Indeed, AtMs in HCV-CV produced somatically mutated RF autoantibodies,[16] and are not removed from the B cell repertoire. However, it remains unclear why only some HCV-infected individuals develop CV, and why anergic mechanisms fail to prevent the development of non-Hodgkin's lymphoma in some patients with HCV-CV.

In this work, we characterized the mechanisms by which AtMs participate in HCV-associated autoimmunity. We show that TLR9-stimulated AtMs secrete TNFα and IgMs with RF activity in patients with HCV-CV. Stimulated AtMs have a specific transcriptional signature centred on TNFα overexpression, which promotes the activation of Th1 cells and conversely reduce Treg proliferation. We found that AtM antibodies did not cross-react against HCV antigens but possessed RF activity. Taken together, our data suggest a central role for TLR9 signalling in AtMs, in driving the breakdown in tolerance that underlies HCV-CV development.

Patients and methods

Patients

Twenty patients with HCV-CV and 10 patients with HCV were included (Table 1). All had positive HCV RNA. HCV viral load was quantified using the Abbott HCV RealTime assay (Abbott) with a lower detection limit of 12 IU/ml. Patients with active HCV vasculitis were defined clinically as previously described.[17] The study was approved by the institutional ethics committee of La Pitié-Salpetrière Hospital and was performed in accordance with the Declaration of Helsinki. All participants provided informed consents.

Cell isolation

Peripheral blood mononuclear cells (PBMCs) were obtained by Ficoll-separation, and $CD19^+IgM^+CD27^+CD21^{-/low}$ (AtM), $CD19^+IgM^+CD27^+CD21^+$ memory B cells, $CD4^+CD25^-$ effector T cells and $CD4^+CD25^{hi}CD127^{-/low}$ regulatory T cells were isolated by FACS using a FACSAria instrument (Becton Dickinson). Flow cytometric analysis of isolated B and T cell subpopulations consistently showed purity of >95%.

Cell culture

Purified B and T cells were cocultured in complete RPMI1640-L-glutamine, and supplemented with 10% FBS and penicillin/streptomycin (100 U/mg/ml) (Sigma-Aldrich). Isolated $CD4^+CD25^-$ effector T cells or $CD4^+CD25^{hi}CD127^{-/low}$ regulatory T cells were cultured for 72 h either alone or 1:1 with sorted AtMs and stimulated with human T-activator CD3/CD28 (Dynabeads) in the presence or absence of 1 μg/ml CpG (Invivogen). For cytokine detection IFNγ, TNFα and IL-17A among $CD4^+CD25^-$ effector T cells in co-culture with AtMs stimulated or not by CpG, PMA (50 ng/ml), ionomycin (250 ng/ml) (Sigma-Aldrich), and brefeldin A (BD Biosciences) were added for the last 6 h of culture.

Table 1. Demographic and clinical characteristics of patients with active HCV-CV or HCV alone.

Characteristics	HCV-CV, n = 20	HCV, n = 10
Age, years	57 [51–64]	54 [48–60]
Male gender (n, %)	11 (55)	6 (60)
HCV genotype (n, %)		
1	12 (60)	6 (60)
2	1 (5)	1 (10)
3	2 (10)	1 (10)
4	5 (25)	2 (20)
5	0	0
Metavir liver fibrosis score (n, %)		
Stage 1	1 (5)	2 (20)
Stage 2	6 (30)	3 (30)
Stage 3	4 (20)	2 (20)
Stage 4	9 (45)	3 (30)
Baseline HCV RNA (log_{10} IU/ml)	5.4 [4.8–6.5]	5.9 [5.6–6.2]
ALT level (IU/L)	67 [41–79]	55 [49–61]
Serum cryoglobulin level (g/L)	0.37 [0.16–0.89]	n.a.
Serum C4 level (g/L)	0.07 [0.03–0.15]	n.a.
Serum rheumatoid factor level (IU/ml)	31 [11–79]	n.a.
Purpura (n, %)	17 (85)	n.a.
Skin ulcer (n, %)	3 (15)	n.a.
Polyneuropathy (n, %)	11 (55)	n.a.
Kidney involvement (n, %)	5 (25)	n.a.

Values are expressed as medians [IQR].
ALT, alanine aminotransferase; HCV, hepatitis C virus; n.a., not applicable.

T cell proliferation assay

Following FACS sorting, T cells were loaded with 0.4 mM CFSE (Thermo Fisher Scientific) for 5 min at 37 °C and cultured as previously described.[11,17] Cultured $CD4^+CD25^{hi}CD127^{-/low}$ regulatory T cells were analysed for cell division using flow cytometry after 72 h of co-culture with AtMs stimulated with CpG 1 mg ODN 2006 Type B CpG oligonucleotide - Human TLR9 ligand (InvivoGen). The concentration of CpG was 1 μg/ml. We used anti-TNFα (Thermo Fisher, clone 28401) at 0.05 μg/ml.

Flow cytometry analysis

PBMCs were stained for 30 min at 4 °C with the following mouse monoclonal antibodies: for B cells; FITC- or PCy7-conjugated anti-CD21, PE- or APC-conjugated anti-CD27, APC-conjugated anti-IgM, energy-coupled dye (ECD)–conjugated anti-CD19, vioblue–conjugated anti-IgD, PCy7-conjugated anti-CD11c, APC-conjugated anti-CD95, FITC-conjugated anti-CD80, APC-conjugated anti-CXCR5, PCy7-conjugated anti-CD38, PE-conjugated anti-CD73, PE-conjugated anti-FCRL3 and anti-FCRL5. T-bet intracellular staining was performed using the PerFix–NC kit (Beckman Coulter) and (PB)-conjugated anti-T-bet antibodies; for T cells, PerCP–conjugated anti-CD4, PE-conjugated anti-CD25, and brillant violet 510–conjugated anti-CD127 (BioLegend). A live/dead discriminant dye was used in accordance with the manufacturer's instructions (Invitrogen). Cells cultured for 72 h were stained for cell surface markers and

then permeabilized with Cytofix/Cytoperm buffer (BD PharMingen) and stained with FITC-conjugated anti-IFNγ (BD PharMingen), PE-conjugated anti-TNFα, and Alexa Fluor 647–conjugated anti-IL-17A (eBioscience), or with APC-conjugated anti-FoxP3. FACS analyses were performed on a Navios flow cytometer using Kaluza analysis software (Beckman Coulter).

Recombinant Fc antigens

To produce recombinant Fc proteins, synthetic genes coding for the human IgK leader peptide followed by the IgH hinge (H) region, the Ig constant domain 2 (C_H2, with a Cys103Ser mutation) and 3 (C_H3) of human IgG1 and IgG3 were cloned into pcDNA™3.1/Zeo$^+$ expression vector (Thermo Fisher Scientific). To generate swapped IgG1-G3 molecules, the sequences encoding the H-C_H2 and C_H3 domains of IgG1 and IgG3 were interchanged in the respective synthetic DNA constructs. The N297A mutation was introduced by directed-site mutagenesis (QuikChange Site-Directed Mutagenesis Kit; Stratagene). All recombinant Fc were produced by transfection of FreeStyle™ 293-F cells using the PEI method as previously described,[18] and purified using protein G sepharose® 4 fast flow beads (GE Healthcare). The Fc peptides library consisted of 8 amino acids-overlapping 20-mer peptides (n = 23; GenScript HK Limited) encompassing the entire IgG1 Fc region.

Single B cell FACS sorting and expression-cloning of antibodies

PBMCs were stained as described, and single AtMs were sorted into 96-well PCR plates using a FACS Aria III sorter (Becton Dickinson) as previously described.[19,20] Single-cell cDNA synthesis using SuperScript III™ reverse transcriptase (Fisher Scientific) followed by nested-PCR amplifications, sequencing and gene analyses were performed as previously described.[19,20] IgH mutations selection strengths were determined using the BASELINE program (http://selection.med.yale.edu/baseline/).[21,22] The IgM- and IgM Fab-expression vectors (Igμ and Igμ-Fab, respectively) were generated from the original IgG1-expression vector[20] by substituting the DNA sequence coding for the constant region of IgG1 by the one of the IgM CH1 followed by an hexahistine tag or of the full IgM (synthetic DNA fragment, GenScript HK Limited).[18,20] Purified digested PCR products were cloned into expressing vectors, and then used to co-transfect FreeStyle™ 293-F cells as previously described.[18,19,20,23] For recombinant IgM production, the co-transfection of Expi293 cells with IgM and IgL (1 μg/ml) and J-chain (2.5 μg/ml) expression vectors was performed using the Expi293™ expression system (Thermo Fisher Scientific). Culture supernatants were harvested 5-days post-transfection and concentrated by centrifugation cycles using Vivacell 100 ultrafiltration units (Sartorius). IgM concentration was determined by ELISA as described previously for IgG.[18] Human IgG antibodies and Fab fragments were purified by affinity chromatography using protein G sepharose® 4 fast flow and Ni sepharose® excel beads (GE Healthcare), respectively. Antibody concentrations were determined using the NanoDrop™ 2000 instrument (Thermo Fisher Scientific).

ELISAs

Polyreactivity and HEp-2 ELISAs were performed as previously described.[24] For Fc-binding experiments, high-binding 96-well ELISA plates (Costar) were coated overnight with 15 μg/well of purified recombinant human IgG-Fc fragments. After washing with 0.05% Tween-PBS (PBST), plates were blocked for 2 h with 2% BSA, 1 mM EDTA, PBST (Blocking buffer). After washing, coated plates were incubated for 2 h with antibodies and 7 consecutive 1:2 dilutions in PBS. After washing, the plates were revealed by incubation for 1 h with HRP-conjugated goat anti-human Kappa light chain (1:10,000; Bethyl laboratories), and by adding 100 μl of HRP chromogenic substrate (ABTS solution, Euromedex). For competition experiments, Fc-coated plates were blocked for 2 h, washed and then incubated for 2 h with recombinant IgM in 1:2 serially diluted solutions of purified protein A (Sigma). Plates were developed, as described, to test the binding of Fabs to IgG1 Fc, Briefly, plates were coated overnight with 0.5 μg/well of purified Fabs in PBS. Plates were then washed, blocked and incubated for 2 h with purified Fc at 50 μg/ml and 7 consecutive 1:2 dilutions in PBS. Plates were revealed as previously described.[24] IgG and IgM reactivity to IgG1 Fc peptides was tested as previously described.[25] For HCV binding experiments, antibodies were tested using the ELISA Kit for Hepatitis C Virus (Amsbio).

Immunoblotting

Purified human Fc fragments were separated by SDS-PAGE with a NuPAGE® 4–12% Bis-Tris Gel (Invitrogen), and electrotransferred onto nitrocellulose membranes. The filters were then saturated for 2 h in PBS-0.05% Tween 20 (PBST)-5% dry milk (blocking buffer) and incubated for 2 h with antibodies (at 30 μg/ml) in blocking buffer. After washing with PBST, filters were incubated for 1 h with 1/5,000-diluted peroxydase-conjugated goat anti-human Kappa light chain (Jackson ImmunoResearch) in blocking buffer. After washing, filters were revealed by chemiluminescence reaction (ECL Prime, GE Healthcare), and images were acquired using a G:Box imaging system (Ozyme).

Indirect immunofluorescence assay

Recombinant antibodies (150 μg/ml), and control antibodies (mGO53,[19] ED38,[26] and internal controls in the kit) were analysed by indirect immunofluorescence assay on HEp-2 cells (ANA AeskuSlides®, Ingen) using the fluorescence microscope Axio Imager 2 (Zeiss) as previously described.[24]

Gene expression profile analysis

RNA was extracted from 10^5–10^6 batch-sorted AtMs, stimulated or not with CpG for 72 h, using the NucleoSpin® RNA II kit (Macherey-Nagel). The quality of the purified RNA was assessed with a 2100 Bioanalyzer (Agilent). Using the Illumina™ TotalPrep™ RNA Amplification Kit (Applied Biosystems), 100 ng RNA was amplified and labelled to produce cDNA. Labelled cDNA was hybridized on whole human genome chips (Human HT-12 Expression BeadChip Kit; Illumina). Data derived from 3 donors were normalized using BeadStudio and bioinformatics analysis was performed using GeneSpring GX 7.3 (Agilent). Probes with a signal <20 were excluded. Differential gene expression was defined according to the following criteria: Among the 48,614 probesets, 1,664 probesets were differentially regulated according to a paired-test with p <0.05 and a false discovery rate (Benjamini Hochberg) p <0.05. We then selected the 251 probesets (=219 genes) with an absolute fold-change of 2. Functional enrichment and network analysis were performed with Ingenuity Pathway Analysis IPA® (QIA-

GEN). For functional analysis, we selected function according to the *p* values and the Z-score to improve biological relevance.

Statistics

Analyses were performed using GraphPad Prism 6.0 software (GraphPad Software). Except where indicated otherwise, values were expressed as mean ± standard deviation (SD). Categorical variables were compared using the Fisher's exact or Chi-square tests, and continuous variables were compared using the 2-tailed Mann-Whitney *U* test. Multiple comparisons with more than 2 groups were performed using the Kruskal-Wallis test with *p* values adjusted by the Bonferroni test (Dunn's method).

Results

Tbet$^+$CD11c$^+$CD27$^+$CD21$^-$ atypical memory B cell expansions in HCV-CV

Expansions of AtMs were previously identified in HCV-CV.[11,12] The patients with HCV-CV examined here (Table 1), also displayed an increased frequency of AtMs (CD27$^+$CD21$^-$ B cells) compared to patients with HCV without CV (28% [±4.9] *vs.* 8.3% [±1.9], $p = 0.008$), and healthy donors (HDs) (2.8% [±0.2], $p = 0.001$) (Fig. 1A, $p = 0.0005$). A significant decrease in AtM frequency was also observed (47 [±5] *vs.* 21 [±5], $p = 0.015$) after CV remission following 12 weeks of direct-acting antiviral (DAA) therapy (Fig. 1B). Although the frequency of AtMs decreased, no significant change in AtM surface marker expression was observed following DAA therapy (Fig. S1). AtMs were the main subpopulation among Tbet positive CD19$^+$ B cells in patients with HCV-CV, but not in HCV controls and HDs (Fig. 1C, $p = 0.0003$) (49% [±5.8] *vs.* 21% [±1.15] and 16% [±5.8]). Tbet positive CD19$^+$ B cells exhibited a differential expression of surface molecules involved in T cell-B cell interactions compared to "classical" CD27$^+$CD21$^+$ resting memory B cells (RMs) (Fig. 1D-E). HCV-CV AtMs showed significantly higher expression of CD11c (1.6 [±0.2] *vs.* 0.91 [±0.07], $p = 0.01$), CD95 (2.8 [±0.2] *vs.* 2 [±0.2], $p = 0.04$) and FCRL5 (1.17 [±0.2] *vs.* 0.55 [±0.18], $p = 0.01$) and decreased expression of CD73 (0.28 [±0.05] *vs.* 0.59 [±0.08], $p = 0.003$) and CXCR5 (18 [±1] *vs.* 29 [±2], $p = 0.003$) compared to RMs. CD80 and FCRL3 expression tended to be higher in AtMs than RMs, while CD38 expression was decreased in AtMs compared to RMs (Fig. 1D-E). Thus, AtMs in HCV-CV share common phenotypic features with AtM subsets described in other chronic infections, autoimmune diseases and healthy individuals.[27–29] We further compared the expression of these surface molecules on AtM and RM subpopulations between HCV-CV, HCV controls and HD. We found higher CD95, CD11c and CXCR5 expression in AtMs and RMs in patients with HCV-CV compared to HCV controls and HDs (AtMs: 2.8 [±0.2] *vs.* 1.2 [±0.5], $p = 0.03$ *vs.* 1.4 [0.1], $p = 0.007$; 1.6 [±0.2] *vs.* 0.7 [±0.05], $p = 0.004$ *vs.* 0.9 [±0.2]; 18 [±2] *vs.* 6 [±0.7], $p = 0.009$ *vs.* 5 [±0.8], $p = 0.02$) (RMs: 2 [±0.2] *vs.* 0.8 [±0.3], $p = 0.02$ *vs.* 0.6 [±0.08], $p = 0.005$; 0.9 [±0.07] *vs.* 0.4 [±0.02], $p = 0.004$ *vs.* 0.5 [±0.09], $p = 0.03$; 29 [±1.3] *vs.* 11 [±2], $p = 0.005$ *vs.* 12 [±1.8], $p = 0.005$). CD80 expression was significantly lower in AtMs and RMs of patients with HCV-CV compared to HCV controls and HDs (AtM 0.9 [±0.09] *vs.* 1.4 [±0.007], $p = 0.03$ *vs.* 1.9 [±0.2], $p = 0.007$; RM 0.7 [±0.05] *vs.* 1.2 [±0.2], $p = 0.02$ *vs.* 1.1 [±0.03], $p = 0.002$). We found no difference in the expression of CD73 and CD38 between AtM and RM subpopulations in HCV-CV, HCV controls and HDs (Fig. S2).

TLR9 signalling in HCV-CV AtMs promote pro-inflammatory Th1 response

TLR9 stimulation can lead to B cell dysfunction in autoimmune diseases.[30,31] Stimulation with TLR9 ligand (*i.e.*, CpG) of sorted AtMs from patients with active HCV-CV enhanced their secretion of TNFα (0.4% *vs.* 8.8%, $p = 0.0003$), but not of IL2, IL6 and IL10 (Fig. 2A, $p = 0.75$). Enhanced secretion of TNFα upon CpG stimulation was significantly higher in AtMs of patients with HCV-CV compared to HCV controls and HDs (8.8 [±1] *vs.* 3.5 [±1], $p = 0.01$ *vs.* 3.5 [±0.5], $p = 0.02$) (Fig. 2A). Stimulation by CpG also increased the proliferation of AtMs (2.5% *vs.* 39.5%, $p = 0.001$) (Fig. 2B, $p = 0.027$), and the production of IgM with reactivity to human IgG1 Fc (Fig. 2C). We next analysed the function of AtMs by studying the expression of CD69, CD25, CD95 and CD44. CD69, CD25 and CD95 expression on AtMs were significantly increased after stimulation by CpG in patients with HCV-CV and HCV controls (5.6 [±0.7] *vs.* 55 [±3.6], $p = 0.0006$, 14 [±2] *vs.* 58 [±2] $p = 0.02$; 9 [±2] *vs.* 44 [±10] $p = 0.002$, 4 [±1] *vs.* 42 [±5] $p = 0.02$; 19.5 [±0.2] *vs.* 61 [±9], $p = 0.04$, 6.9 [±1.3] *vs.* 23 [±0.6], $p = 0.02$) (Fig. 2D, respective *p* values for the expression of CD69, CD25, CD95 and CD44 were 0.43, 0.72, 0.86 and 0.95). Stimulation of AtM cells with CpG has no significant impact on CD44 expression in patients with HCV-CV (Fig. 2D). Th1 cells have been shown to be involved in the pathogenesis of HCV-CV.[9,32] We therefore evaluated whether AtMs can control the release of pro-inflammatory cytokines by CD4$^+$CD25$^-$ effector T cells (Teffs) in patients with HCV-CV. Sorted AtMs stimulated or not with CpG were cocultured with autologous CD4$^+$CD25$^-$ T cells. The presence of AtMs stimulated with CpG cocultured with autologous CD4$^+$CD25$^-$ T cells tended to increase IFNγ (Fig. 3A, $p = 0.028$) and TNFα (Fig. 3B, $p = 0.013$) production by autologous CD4$^+$CD25$^-$ T cells, but did not significantly affect IL17A expression (Fig. 3C, $p = 0.73$). Functional defects of Tregs contribute to HCV-CV-associated autoimmune manifestations.[6,33,34] However, it is still unclear whether clonally expanded AtMs contribute to the perturbations in T cell homeostasis in HCV-CV. CpG-stimulated AtMs were cocultured with autologous Teffs or Tregs stimulated with anti-CD3/CD28. CpG-stimulated AtMs reduced Treg proliferation (83% *vs.* 44%, $p = 0.036$), and increased Teff proliferation (81% *vs.* 89%, $p = 0.01$) (Fig. 3D,E). Thus, TLR9 signalling in AtMs promotes the proliferation and secretion of IFNγ and TNFα but not IL17A by Teffs, and reduces the proliferation of Tregs in HCV-CV. The addition of anti-TNFα in the co-culture significantly decreased IFNγ and TNFα secretion by Teffs but did not impact Treg proliferation (Fig. 3A,B). No significant changes in the expression of functional markers of Tregs (CTLA4, ICOS and PD1) were observed when stimulated AtMs were cocultured with Tregs (data not shown).

Stimulated HCV-CV AtMs harbour a specific TNFα-centred transcriptional profile

Transcriptional profiling of HCV-CV AtMs previously revealed an association with molecular pathways involved in anergy, apoptosis, and dampened activation of B cells.[11,13] To define gene signatures associated with the effect of TLR9 stimulation on AtMs, we compared gene expression profiles of CpG-stimulated and unstimulated AtMs (control) from patients with HCV-CV (Fig. 4). We identified a gene signature of 229 genes in total (210 upregulated and 19 downregulated) in CpG-stimulated AtMs compared to controls (Fig. 4A). Functional enrichment analysis in CpG-stimulated AtMs revealed many

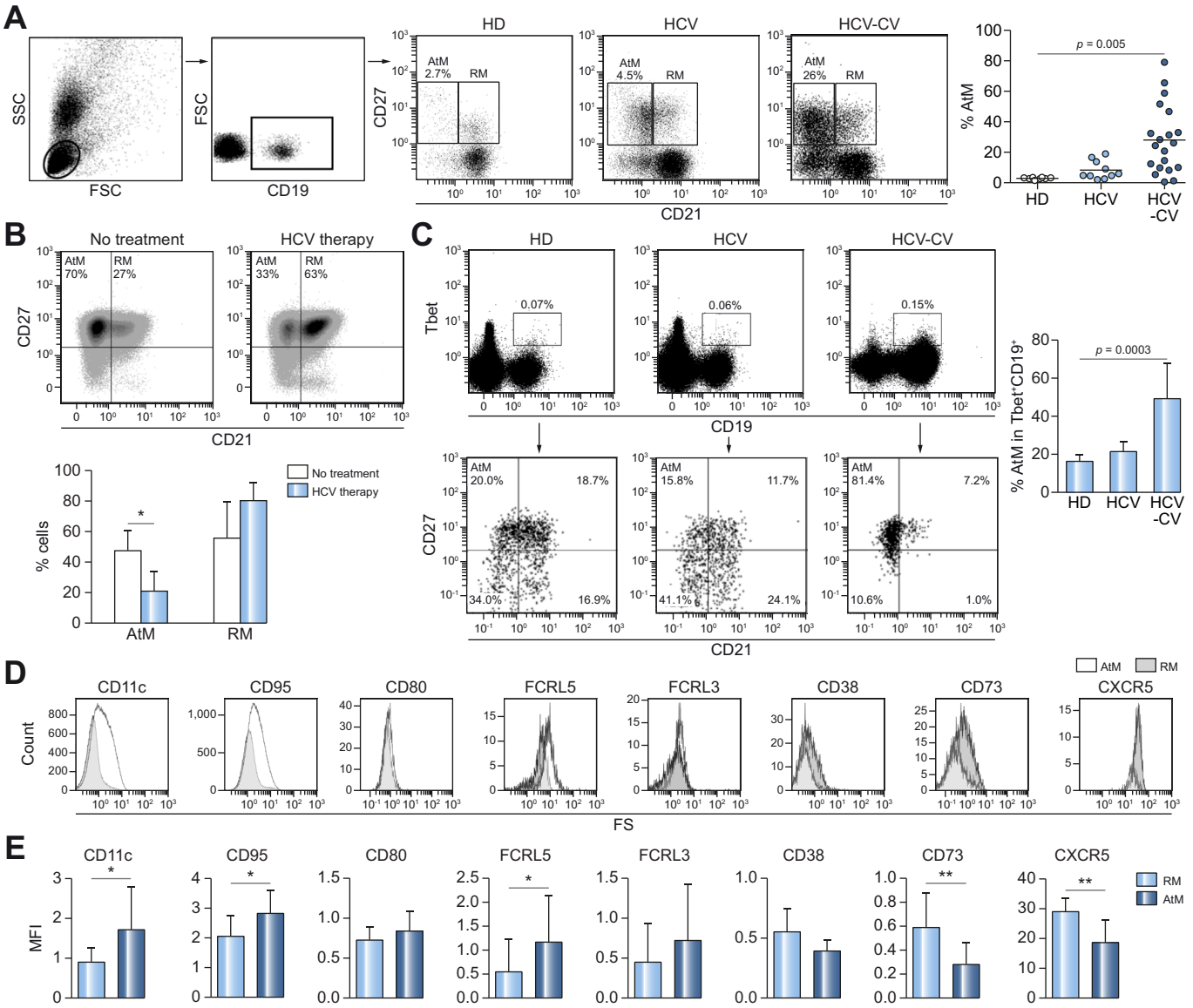

Fig. 1. Immunophenotyping of expanded AtMs in patients with HCV-CV. (A) Representative flow cytometry plots showing the frequency of $CD27^{+}CD21^{-}$ B cells (AtMs) in patients with HCV-CV compared to HCV-infected controls without CV and HD. Dot graph showing the frequency of AtM in 20 patients with HCV-CV, 10 HCV controls and 8 HD (right). (B) Flow cytometry plots showing AtM and RM frequency in patients with HCV-CV before and 12 weeks after HCV therapy (upper). Bar graph showing AtM and RM count changes upon HCV treatment in 6 patients with HCV-CV (lower). (C) Representative flow cytometry plots showing Tbet expression among B cells (upper panels) and AtM frequency among $Tbet^{+}CD19^{+}$ cells (lower panel) in patients with HCV-CV, HCV controls and HD. Bar graph presenting percentage of AtM^{+} $Tbet^{+}CD19^{+}$ cells in 6 HD, 10 HCV controls and 10 patients with HCV-CV (right). (D) Flow cytometry histograms showing the differential expression of surface markers between AtM and $CD27^{+}CD21^{+}$ RMs from representative HCV-CV patient. (E) Bar graphs presenting the comparison of the surface markers expression showed in D between AtM and RM cells measured in 9 patients with HCV-CV. Mean values ± SD are given. Mann-Whitney test was used to compare differences between 2 groups (Fig. 1B and 1E). Multiple comparisons with more than 2 groups were performed using the Kruskal-Wallis test with *p* values adjusted by the Bonferroni test (Dunn's method), in Fig. 1A and 1C. $^{*}p$ <0.05; $^{**}p$ <0.01. AtMs, atypical memory B cells; HCV-CV, HCV-associated cryoglobulinaemia vasculitis; HD, healthy donors; RMs, resting memory B cells.

upregulated genes that are involved in B- and Th1-cell activation (Fig. 4B). Among the top upregulated genes, we found high expression of *MIR155HG* which codes for miRNA-155. miRNA-155 influences BCR signalling and is highly expressed on activated B cells,[35] contributing to a breakage in tolerance when induced in B cells upon TLR9 signalling.[30] Interestingly, the pro-inflammatory cytokine MIF, which drives the Th1 response,[36] was also highly expressed in CpG-stimulated AtMs. We then focused on the molecular networks showing the most induced genes as a group in CpG-stimulated AtMs (Fig. 4C). The gene content of this transcriptional module was enriched in genes encoding proteins involved in B cell activation and differentiation, signal transduction and in T cell co-stimulation, such as TNFα, interferon regulatory factor-4 (*IRF4*), BLIMP1 (*PRDM1*), and *STAT3* genes (Fig. 4C). Among the top genes downregulated, we identified *FAIM3* that encodes an IgM Fc receptor, and which may serve as an uptake receptor for IgM-opsonized antigens by B cells.[37] Hydrogen voltage-gated channel 1 (*HVCN1*) coding for a voltage-gated proton channel and C8orf13-BLK (src family tyrosine kinase) were also downregulated in CpG-stimulated AtMs. Interestingly, *HVCN1*-deficient mice exhibit autoimmune phenotypes including splenomegaly, nephritis, and autoantibody

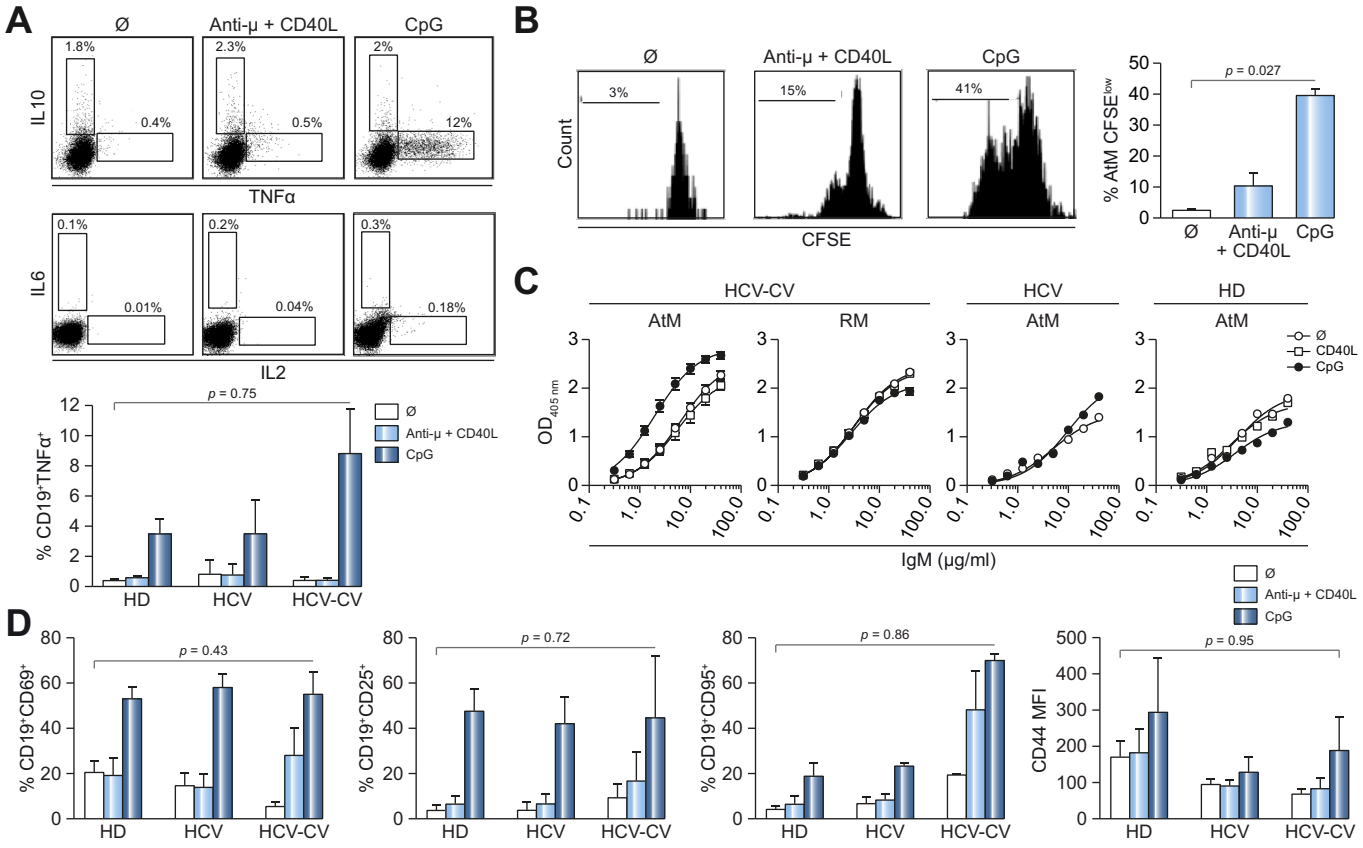

Fig. 2. Effects of TLR9 signalling on AtMs in patients with HCV-CV. (A) Representative flow cytometry plots show the percentage of AtMs from patients with HCV-CV alone and stimulated (anti-mu + CD40L, or CpG) positive for the different cytokines measured (upper panel). Bar graph comparing the mean percentage of TNFα$^+$ AtMs in the 3 culture conditions measured for 4 HD, 4 HCV controls and 7 HCV-CV donors (lower panel). Error bars indicate the SD. (B) Same as in (A) but for the % of proliferating AtMs. (C) Representative ELISA graph comparing the IgG1-Fc reactivity of IgM produced in the supernatant of AtM or RM from patients with HCV-CV and AtM from HCV controls and HD cultured alone and in the presence of CD40L and CpG. (D) Bar graphs presenting different expression of surface markers on AtMs of HD (n = 4), HCV controls (n = 4) and patients with HCV-CV (n = 7) cultured alone and stimulated (anti-mu + CD40L or CpG). Mean values ± SD are given. Multiple comparisons with more than 2 groups were performed using the Kruskal-Wallis test with *p* values adjusted by the Bonferroni test (Dunn's method). AtMs, atypical memory B cells; HCV-CV, HCV-associated cryoglobulinaemia vasculitis; HD, healthy donors; RMs, resting memory B cells.

production.[38] Polymorphisms of C8orf13-BLK are associated with autoimmune diseases.[39–41] Altogether, these data suggest that the activation of AtMs through TLR9 signalling could lead to a Th1 pro-inflammatory state, which could facilitate the breakdown in tolerance in HCV infection.

AtMs display antigen-driven maturation features

To characterize the antibody repertoire and reactivity of AtMs, we isolated single circulating blood AtMs from 3 donors (Fig. 5A), amplified and sequenced their heavy- and light-chain variable domain (IgH and IgL, respectively) genes. We found that most if not all captured AtMs belong to unique clonal families (96 to 100%) (Fig. 5B), characterized by various degrees of clonal diversity depending on the donor (Fig. 5C). Clonally expanded B cells in donor patient 1 expressed IgMs encoded by V_H1-69/D_H3-10/J_H4 and Vκ3-20/Jκ2 rearrangements (Fig. 5D). Interestingly, patient 2 and patient 3 donors showed clonal expansions of AtMs with very similar recombined IgH and IgL. Both used V_H3-7 and J_H3 genes with a D_H3-10 or D_H3-22 segment, and Vκ3-15 and Jκ1 genes (Fig. 5D). AtM antibodies displayed moderate to relatively high levels of somatic mutations in IgH and IgL variable genes (Fig. 5E). Somatic mutations showed a strong selection of replacement mutations in complementarity-determining regions compared to framework regions (Fig. 5F), suggesting that anergic AtMs were shaped following an antigen-driven affinity maturation process.

AtM antibodies are rheumatoid factors lacking HCV reactivity

To identify the antigen specificities of HCV-CV AtM antibodies, we produced recombinant monoclonal antibodies that were representative of each clonal expansion (Fig. 5C). IgM expressed by clonally expanded anergic AtMs has been shown to exert RF activity.[16] All recombinant IgM antibodies recognized the human IgG1 Fc fragment (IgG1-Fc) (Fig. 6A), confirming their RF activity. Fab fragments of parental IgM but not IgG counterparts bound to IgG1-Fc, which may be explained by self-competition for RF binding sites when the full IgG molecule is expressed in complex with its own Fc. They also reacted against IgG1-Fc by immunoblotting (Fig. 6B) but not against any of the overlapping peptides covering the entire Fc region (Fig. 6C), suggesting that the epitopes recognized by AtM antibodies are conformational. Moreover, we assessed whether unresponsive RF-expressing AtMs display auto- and polyreactive properties. ELISA binding experiments showed that IgG and IgM RF antibodies exhibit neither polyreactivity nor self-reactivity against HEp-2 cell antigens (Fig. 6D). Cross-reactivity of RF antibodies against HCV antigens has been suggested,[42–44] but never for-

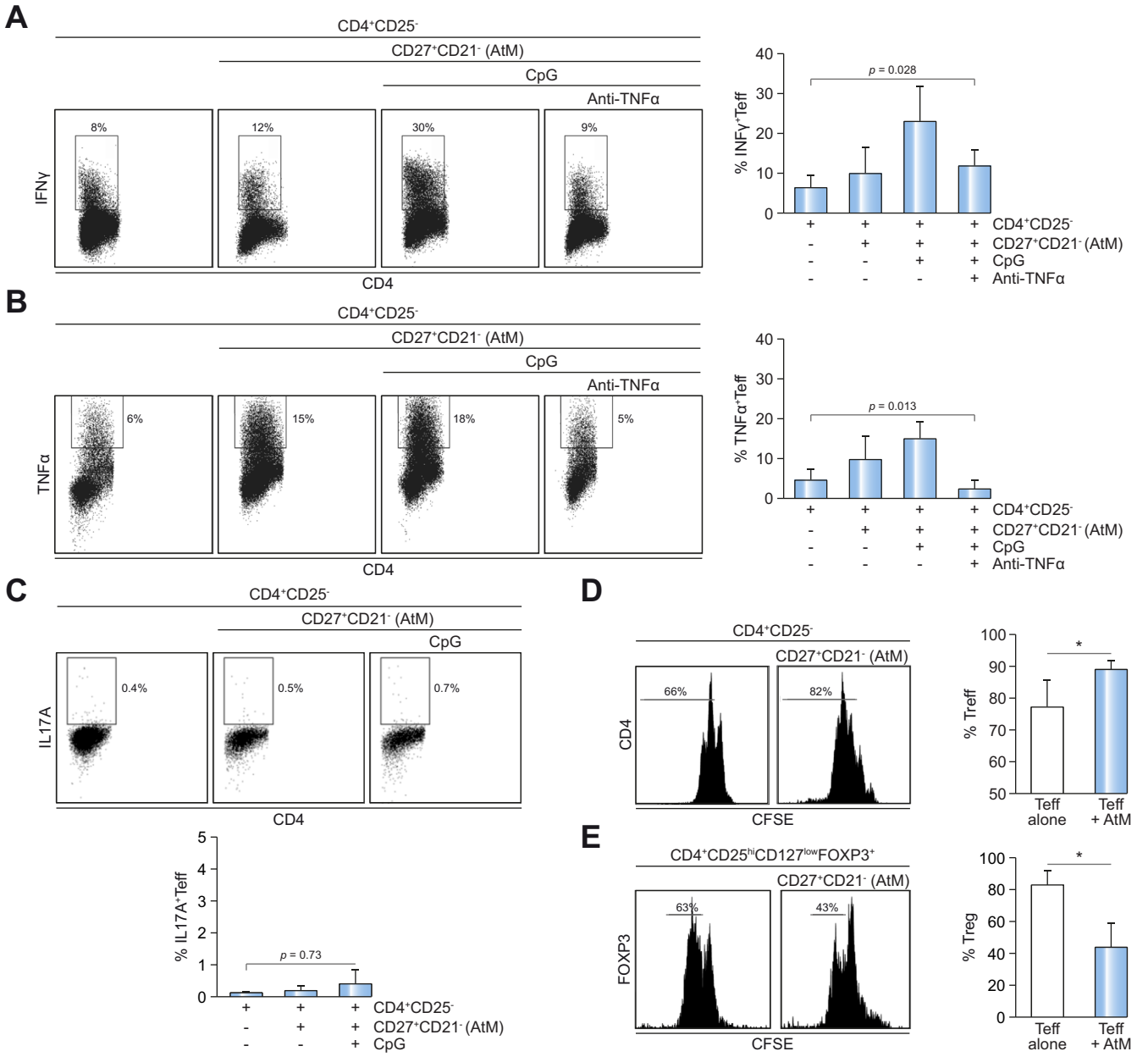

Fig. 3. Effects of CpG-stimulated AtMs on effector and regulatory T cell subsets. (A) Representative flow cytometry plot shows the percentage of $CD4^+IFN\gamma^+$T cells alone and after co-culture with AtMs stimulated or not with CpG and with the addition of anti-TNFα in the co-culture (left). Bar graph comparing the mean percentage of $CD4^+IFN\gamma^+$T cells in the 4 culture conditions measured for 6 patients with HCV-CV (right). Error bars indicate the SD. (B) Same as for (A) but for the mean percentage of $CD4^+TNF\alpha^+$ T cells. (C) Same as for (A) but for the mean percentage of $CD4^+IL17A^+$ T cells measured for 6 patients with HCV-CV. (D) Representative flow cytometry histogram shows the CFSE proliferation of sorted $CD4^+CD25^-$ T cells alone or in co-culture with AtMs from patients with HCV-CV (top). Bar graph comparing the mean percentage of proliferating $CD4^+CD25^-$ T cells (Teff) alone or co-cultivated with AtMs for 6 patients with HCV-CV (bottom). Error bars indicate the SD. (E) Same as for (D) but for the mean percentage of proliferating $CD4^+CD25^{hi}CD127^{low}FOXP3^+$ T cells (Treg). Mean values ± SD are given. Mann-Whitney test was used to compare differences between 2 groups (Fig. 3D and 3E). Multiple comparisons with more than 2 groups were performed using the Kruskal-Wallis test with *p* values adjusted by the Bonferroni test (Dunn's method), in Fig. 3A, 3B and 3C). **p* <0.05. AtMs, atypical memory B cells; HCV-CV, HCV-associated cryoglobulinaemia vasculitis; Teff, effector T cells; Treg, regulatory T cells.

mally demonstrated. ELISA binding analysis showed that none of the recombinant antibodies recognized HCV NS3-5, Core, or E2 proteins (Fig. 6E).

AtM antibodies recognize distinct IgG-Fc epitopes

To define more precisely the epitopes targeted by AtM-derived RF, we first investigated the potential role of Fc-associated *N*-glycans. Antibody binding analyses showed that IgM reactivity was not affected by the absence of *N*-glycans in position N297 (Fig. 7A). Since the association of *Staphylococcus aureus* protein A with Fc protein was previously shown to interfere with HCV-associated RF reactivity,[16] we next assayed the IgM binding to Fc in the presence of purified protein A. Competition ELISA analyses indicated that protein A could block or decrease the Fc-binding by representative IgMs from patient 1 and patient 2 but not from patient 3 (Fig. 7B). Finally, we compared IgM binding to IgG1, IgG3 and hybrid Fc molecules made up of the H-CH2 of IgG1 followed by the CH3 of IgG3, and *vice versa*. Our results showed that 1-04 bound preferentially to IgG1 and hybrid Fc proteins and to a lesser extent to IgG3 (Fig. 7C). The

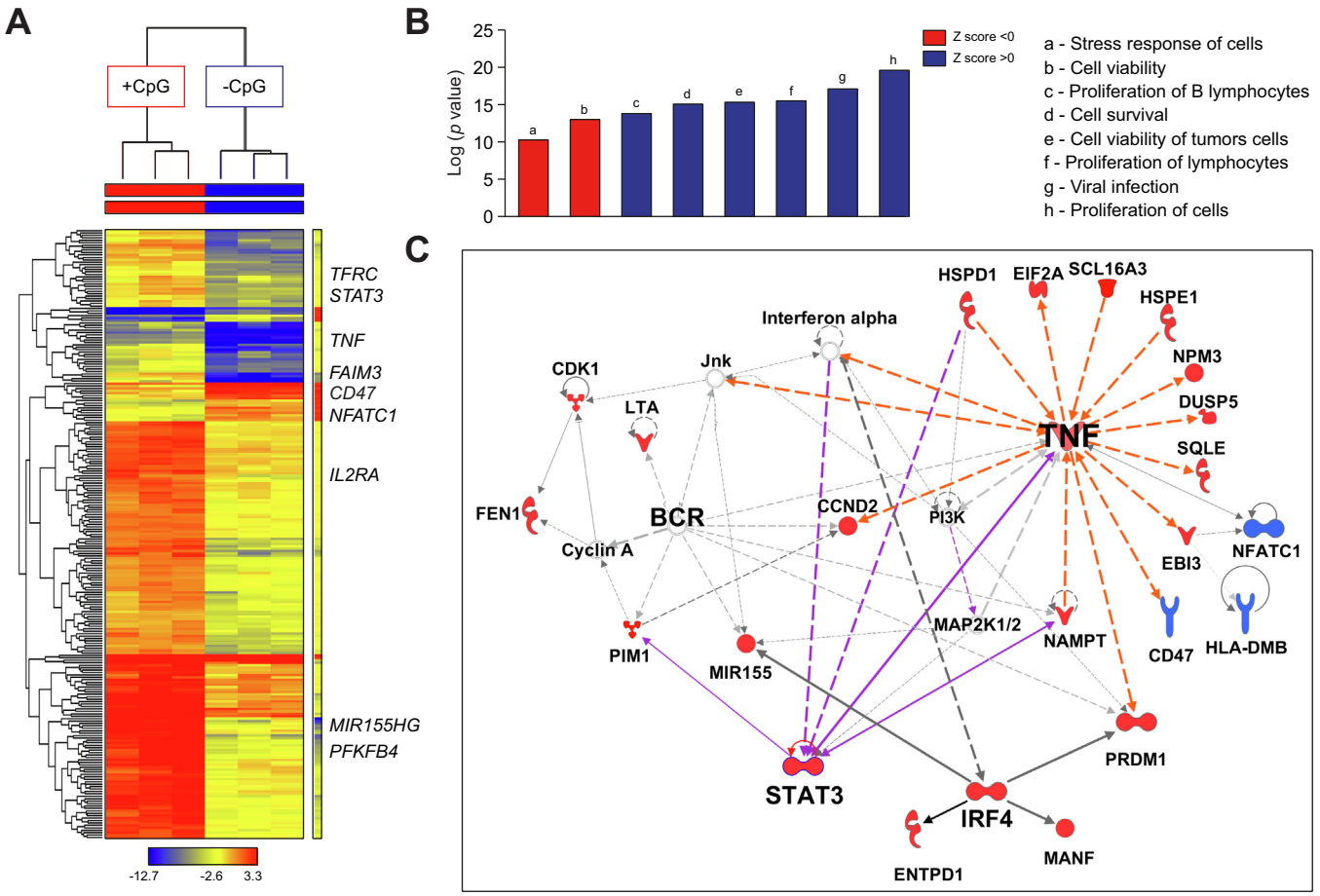

Fig. 4. Gene profiling of HCV-CV AtMs in response to TLR9 stimulation. (A) Heatmap showing the differential expression (fold-change >2) of 219 genes between unstimulated and CpG-stimulated AtMs from 3 patients with HCV-CV. (B) Bar graph showing the cellular pathways containing up- (red) and down- (blue) regulated transcripts in CpG-stimulated AtMs. (C) Diagram shows one of the top network, centred on both TNF and STAT3, which was identified by functional enrichment on the top molecular function activated in CpG-stimulated AtMs. Links of up- (red) and down- (blue) regulated genes of the 219 gene signature with TNF and STAT3 molecules are indicated in orange and purple, respectively. AtMs, atypical memory B cells; HCV-CV, HCV-associated cryoglobulinaemia vasculitis. (This figure appears in colour on the web.)

lower affinity variant 1-10 as well as 2-23 and 3-70 only reacted against the entire IgG1 Fc and its CH3 domain on the corresponding hybrid molecule (Fig. 7C). Together, these data suggest that the RF expressed by the expanded clonal AtMs target various epitopes on the human Fc (Fig. 7D).

Discussion

Immune dysregulation in HCV-CV involves expansion of anergic AtMs believed to produce RF autoantibodies.[1,8,16] HCV-CV AtMs have increased levels of molecules involved in T-B cell interactions including CD11c, CD80 and CD86/B7-2.[11,13] AtMs with similar phenotypic features have also been identified in the context of chronic infections,[45–47] in autoimmune diseases,[15,48] and in healthy individuals.[27] We found here that AtMs have higher expression of T-bet, CD11c, CD80, CD95, FCRL3, and FCRL5, and decreased CD73 and CXCR5 surface levels compared to RMs in HCV-CV.[13,49,50] Moreover, T-bet expression in AtMs was enhanced in patients with HCV-CV compared to HCV controls without CV. Interestingly, the expansion of AtMs in patients with HCV-CV decreased significantly after DAA therapy, whereas the expression of AtM surface markers remained unchanged. This is likely a consequence of the antigens' removal, and cessation of chronic viral stimulation of autoreactive AtMs following DAA therapy.

Human AtMs may differ functionally depending on the context of chronic infection or autoimmunity. HIV- and malaria-associated AtMs exhibit markedly reduced cytokine and antibody production capacity,[45,51,52] whereas AtMs found in autoimmune diseases produce pro-inflammatory cytokines and autoantibodies.[53–55] HCV-CV AtMs resemble exhausted cells found in chronic inflammation, which are anergic and lack the potential to differentiate into antibody-secreting cells.[15] However, TLR9 signalling in AtMs could break this anergic state.[56] While such signals would ordinarily trigger apoptosis, cognate T cell help and cytokines such as IFNγ and TNFα could promote autoantibody production.[57] We showed here that stimulation of AtMs by TLR9 ligand CpG drives their differentiation into RF-producing cells. We found that CpG-stimulated AtMs display enhanced TNFα secretion, which is likely responsible for the proliferation and secretion of IFNγ and TNFα by Teffs. The interplay between BCR, TLR9, and cytokine signalling in the generation of T-bet$^+$ CD11c$^+$ B cells has recently been unveiled.[58] In mice, *Plasmodium* DNA-sensing through TLR9 along with IFNγR have been shown to provide an essential synergizing signal for promoting AtM expansion and the subsequent development of autoimmune anaemia.[59] Activation of murine autoreactive RF$^+$ B cells by immune complexes requires the synergistic engagement of the BCR and MyD88-dependent

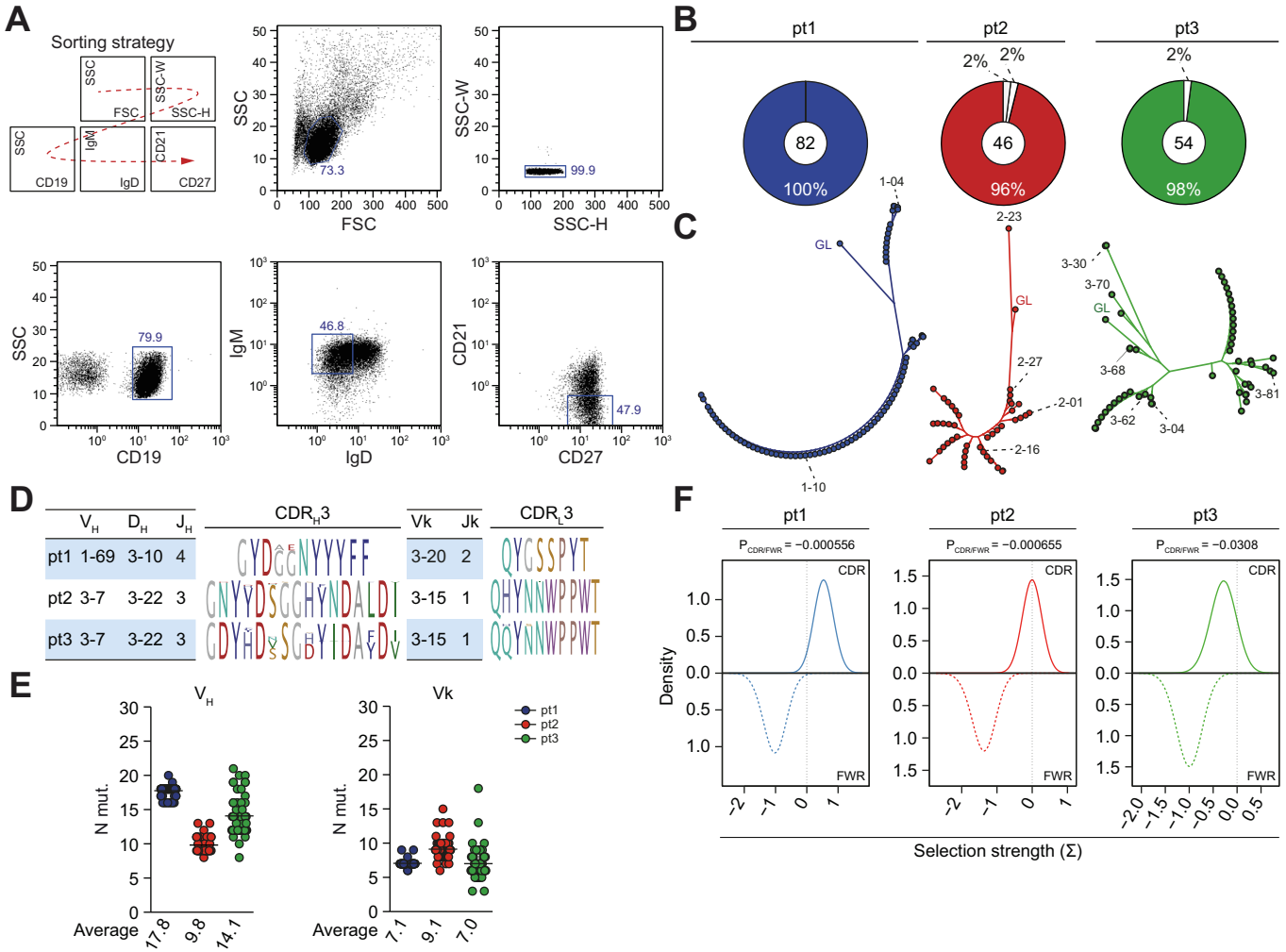

Fig. 5. Immunoglobulin gene repertoire of AtMs. (A) Flow cytometry plots show the staining of patients' PBMCs with fluorescently labelled antibodies used for the identification and single sorting of AtMs. (B) Pie charts show clonal expansions of AtMs isolated from patient 1 (pt1, in blue), patient 2 (pt2, in red) and patient 3 (pt3, in green). The total number of analysed memory B cell antibodies is indicated in the centre, each pie slice represents a clonal family and the area of the slice is proportional to the number of clonal relatives. Each clonal family is represented by the same colour and unique members are not coloured. (C) Phylogenic trees of the AtM clonal expansions. GL, putative germline precursor sequence. Clonal members expressed as recombinant antibodies are indicated on the phylogeny. (D) Schematic diagram indicates the $V_HD_HJ_H$ and VκJκ genes, and IgH/IgL CDR3s as consensus sequences from all the members in each clonal expansion. (E) Dot plots show for each patient, the numbers of mutations in V_H and Vκ genes of AtMs. The average number of mutations is indicated below each dot plot. (F) Graphs show the Bayesian estimation of antigen-driven selection of the Ig sequences in clonal B cell families. Values >0 indicate positive selection. AtMs, atypical memory B cells; PBMCs, peripheral blood mononuclear cells. (This figure appears in colour on the web.)

TLR members (*i.e.*, TLR7, TLR8 and TLR9).[60] These data suggest a critical link between innate and adaptive immune responses in the development of systemic autoimmune diseases, particularly when associated with chronic infections. Thus, consistent with our results, we hypothesize that TLR9 signalling could activate anergic RF-expressing AtMs, which in turn would create a pro-inflammatory environment by favouring a Th1 response. Analyses of the transcriptional program of CpG-activated HCV-CV AtMs provided further evidence supporting this scenario. HCV-CV AtMs were previously shown to be associated with molecular pathways involved in anergy, and dampened activation of B cells via their BCR.[1,4] In contrast, CpG-stimulated AtMs upregulated many genes involved in B cell activation and T-B interactions, and centred on TNFα overexpression. TNFα activates STAT3, a key regulator of B cell proliferation and survival.[61] Higher transcript expression of miRNA-155 and the heat shock proteins (HSP90B1, HSPD1, HSPE1), which are known to induce B cell activation and to disrupt immune tolerance,[8–10] as well as IRF4 and BLIMP1, which promote immunoglobulin production,[62] was also demonstrated in activated AtMs. Moreover, we identified a transcriptomic program in TLR-9-stimulated AtMs that drives T-B cell interactions (TNFα, IRF4, and STAT3) and Th1 pro-inflammatory immune responses (MIF). Taken together, these data suggest that activation of AtMs through TLR9 signalling leads to RF production and a B cell-driven Th1 pro-inflammatory state.

AtMs captured from HCV-CV were part of large single clonal expansions and showed clear evidence of antigen-driven maturation.[11,12,16] AtM-derived recombinant IgM antibodies displayed RF activity with increased binding to IgG-Fc by avidity effects, as shown elsewhere.[16] Fc-binding was not due to polyreactivity and was not associated with additional autoreactivity features. This contrasts with the frequent or predominant poly- and self-reactivity described for the AtM subsets expanded in other infectious and autoimmune diseases.[15,47,63,64] Interestingly, mapping of AtM RFs revealed the diversity of targeted epitopes on the Fc region, with no immunodominance towards a common unique epitope. This is reminis-

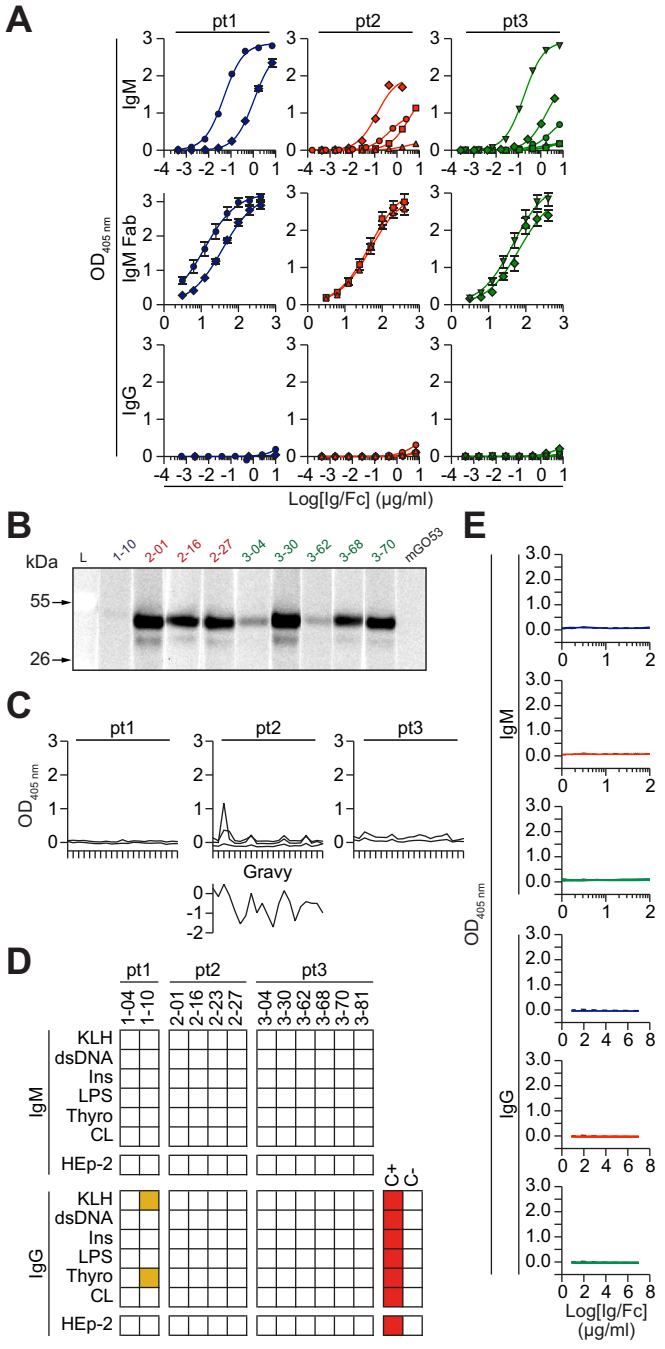

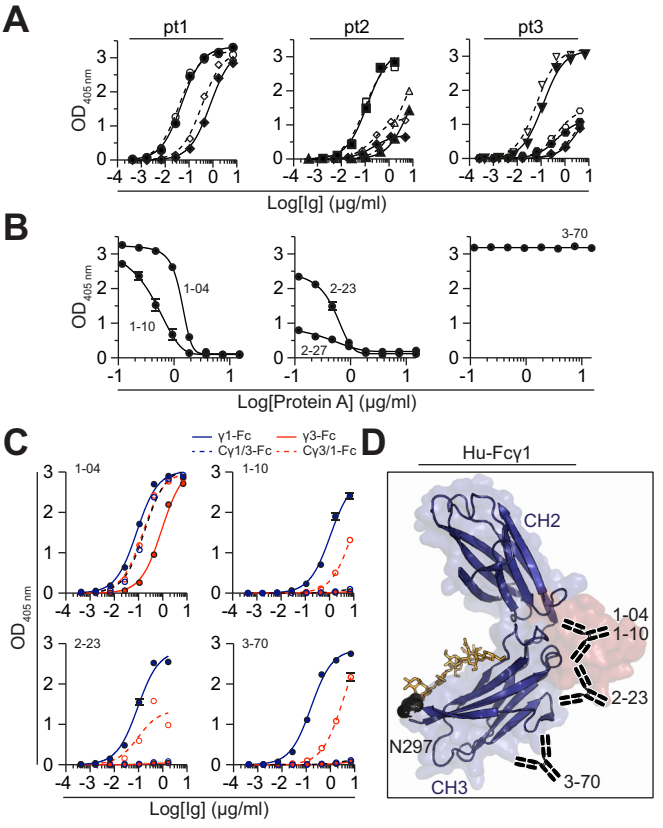

Fig. 6. Antibody reactivities of AtMs. (A) ELISA graphs show the reactivity of AtM antibodies expressed as recombinant IgM, IgG1 and IgM Fab fragments against the human IgG1 Fc. (B) Immunoblotting showing the reactivity of AtM antibodies against the human IgG1 Fc. L, protein ladder indicating molecular masses. (C) Graphs show the ELISA reactivity of IgM antibodies to IgG1-Fc overlapping peptides. The values of grand average of hydropathy (GRAVY) for all peptides are indicated below. (D) Heat map showing the reactivity of AtM IgM and IgG antibodies against various purified antigens and HEp-2 cells lysate to detect polyreactive binding by ELISA. Colour intensity is proportional to the reactivity level with darker red colours indicating high binding while light colours show moderate binding (white = no binding). (E) Graphs show the reactivity of recombinant IgM and IgG AtM antibodies against HCV proteins. AtMs, atypical memory B cells; C+, positive control; C-, negative control; CL, cardiolipid; dsDNA, double-stranded DNA; Ins, insulin; KLH, keyhole limpet hemocyanin; LPS, lipopolysaccharide; Thyro, thyroglobulin. (This figure appears in colour on the web.)

Fig. 7. Mapping of RF epitopes on the human IgG1-Fc. (A) ELISA graphs comparing the binding of selected AtM IgM antibodies to wild-type (straight lines) and N297A mutant (dotted lines) Fc molecules. (B) ELISA graphs show the binding of selected recombinant IgM to human IgG-Fc protein in presence of purified protein A as a potential competitor. (C) ELISA graphs comparing the IgM binding to wild-type human IgG1 and IgG3 Fcs, and to swapped IgG1-3 and IgG3-1 molecules. (D) The schematic diagram (based on the PDB-1FC2 structure[71]) shows putative antibody binding sites on human Fc. Fc *N*-glycans and bound protein A are shown in yellow and red, respectively. AtMs, atypical memory B cells; RF, rheumatoid factor. (This figure appears in colour on the web.)

cent of the epitopic diversity characterizing RFs in rheumatoid arthritis,[65] which probably use different types of interactions for Fc recognition.[66,67] The E2 subunit of the HCV envelope spike contains a β-sandwich element sharing structural homology with immunoglobulin domains.[68] A phenomenon of molecular mimicry between Ig folds of human IgGs and HCV envelope glycoproteins has been proposed to explain the development of RFs in HCV-CV.[42] However, we found that AtM RF IgMs do not cross-react with HCV antigens including the E2 moiety. In line with this, whether antibodies expressed by HCV-associated lymphoma cells, some of which exhibit RF activity, truly recognize the E2 protein remains equivocal.[44,69,70] Thus, IgGs, possibly bound to viral antigens as immune complexes, are most likely the only culprits driving the emergence of clonally expanded B cells with RF activity in HCV-CV.

In conclusion, our results suggest a central role for TLR9 activation of AtMs in breaking tolerance in patients with HCV-CV. Importantly, we showed in HCV-CV that CpG-stimulated AtMs, through the secretion of TNFα, have deleterious effects, by stimulating proliferation and activation of effector Th1 cells, inhibiting Treg proliferation and promoting the production of IgM with

RF activity. RF molecules produced by AtMs recognized distinct IgG-Fc epitopes and did not cross-react against HCV proteins, confirming that molecular mimicry between HCV and human IgG proteins is not the trigger of HCV-associated autoimmunity.

Financial support
This work was supported by the ANRS, France (CSS7 AO 2014-2).

Conflict of interest
The authors declare no competing financial interests, and no personal conflicts of interest.

Please refer to the accompanying ICMJE disclosure forms for further details.

Authors' contributions
H.M. and D.S. conceived the study. D.K., P.C., H.M. and D.S. supervised the work. C.C., V.L., C.M., A-C. D., N.J., C.P., A. M-D., M.T., T.H., V.Q., M.R. and H.M. performed experiments and analysed data. C.C., H.M. and D.S. wrote the manuscript with contributions from all the authors.

Acknowledgements
We are grateful to all participants who consented to be part of this study. We thank Valentina Libri for her assistance with single cell sorting at the Center for Human Immunology (CIH, Institut Pasteur). The authors also thank the UMR 8199 LIGAN-MP Genomics platform (Lille, France), which belongs to the "Federation de Recherche" 3508 Labex EGID (European Genomics Institute for Diabetes; ANR-10-LABX-46) and was supported by the ANR Equipex 2010 session (ANR-10-EQPX-07-01; "LIGAN-MP"). The LIGAN-PM Genomics platform (Lille, France) is also supported by the FEDER and the Region Nord-Pas-de-Calais-Picardie. This work was supported by the ANRS (CSS7 AO 2014-2). H.M. was supported by the G5 Institut Pasteur Program, the INSERM and the Milieu Intérieur Program (ANR-10-LABX-69-01). C.C. was supported by the Fondation pour la Recherche Médicale (FDM20140630463) and C.M. by "Année Recherche de l'Agence Régionale de Santé d'Ile de France" (#2016-11-52).

Supplementary data
Supplementary data to this article can be found online at https://doi.org/10.1016/j.jhep.2019.06.029.

References
[1] Cacoub P, Poynard T, Ghillani P, Charlotte F, Olivi M, Piette JC, et al. Extrahepatic manifestations of chronic hepatitis C. MULTIVIRC Group. Multidepartment Virus C. Arthritis Rheum 1999;42:2204–2212.
[2] Desbois AC, Cacoub P, Saadoun D. Cryoglobulinemia: an update in 2019. Joint Bone Spine 2019, pii: S1297-319X (19)30014-4.
[3] Roccatello D, Saadoun D, Ramos-Casals M, Tzioufas AG, Fervenza FC, Cacoub P, et al. Cryoglobulinaemia. Nat Rev Dis Primer 2018;4:11.
[4] Cacoub P, Renou C, Rosenthal E, Cohen P, Loury I, Loustaud-Ratti V, et al. Extrahepatic manifestations associated with hepatitis C virus infection. A prospective multicenter study of 321 patients. The GERMIVIC. Groupe d'Etude et de Recherche en Medecine Interne et Maladies Infectieuses sur le Virus de l'Hepatite C. Medicine (Baltimore) 2000;79:47–56.
[5] Cacoub P, Comarmond C, Domont F, Savey L, Saadoun D. Cryoglobulinemia vasculitis. Am J Med 2015;128:950–955.
[6] Boyer O, Saadoun D, Abriol J, Dodille M, Piette J-C, Cacoub P, et al. CD4 +CD25+ regulatory T-cell deficiency in patients with hepatitis C-mixed cryoglobulinemia vasculitis. Blood 2004;103:3428–3430.
[7] Lenzi M, Frisoni M, Mantovani V, Ricci P, Muratori L, Francesconi R, et al. Haplotype HLA-B8-DR3 confers susceptibility to hepatitis C virus-related mixed cryoglobulinemia. Blood 1998;91:2062–2066.
[8] Saadoun D, Landau DA, Calabrese LH, Cacoub PP. Hepatitis C-associated mixed cryoglobulinaemia: a crossroad between autoimmunity and lymphoproliferation. Rheumatol Oxf Engl 2007;46:1234–1242.
[9] Saadoun D, Boyer O, Trébeden-Nègre H, Limal N, Bon-Durand V, Andreu M, et al. Predominance of type 1 (Th1) cytokine production in the liver of patients with HCV-associated mixed cryoglobulinemia vasculitis. J Hepatol 2004;41:1031–1037.
[10] Saadoun D, Bieche I, Maisonobe T, Asselah T, Laurendeau I, Piette JC, et al. Involvement of chemokines and type 1 cytokines in the pathogenesis of hepatitis C virus-associated mixed cryoglobulinemia vasculitis neuropathy. Arthritis Rheum 2005;52:2917–2925.
[11] Terrier B, Joly F, Vazquez T, Benech P, Rosenzwajg M, Carpentier W, et al. Expansion of functionally anergic CD21-/low marginal zone-like B cell clones in hepatitis C virus infection-related autoimmunity. J Immunol (Baltim Md 1950) 2011;187:6550–6563.
[12] Charles ED, Green RM, Marukian S, Talal AH, Lake-Bakaar GV, Jacobson IM, et al. Clonal expansion of immunoglobulin M+CD27+ B cells in HCV-associated mixed cryoglobulinemia. Blood 2008;111:1344–1356.
[13] Charles ED, Brunetti C, Marukian S, Ritola KD, Talal AH, Marks K, et al. Clonal B cells in patients with hepatitis C virus-associated mixed cryoglobulinemia contain an expanded anergic CD21low B-cell subset. Blood 2011;117:5425–5437.
[14] Duty JA, Szodoray P, Zheng N-Y, Koelsch KA, Zhang Q, Swiatkowski M, et al. Functional anergy in a subpopulation of naive B cells from healthy humans that express autoreactive immunoglobulin receptors. J Exp Med 2009;206:139–151.
[15] Isnardi I, Ng Y-S, Menard L, Meyers G, Saadoun D, Srdanovic I, et al. Complement receptor 2/CD21- human naive B cells contain mostly autoreactive unresponsive clones. Blood 2010;115:5026–5036.
[16] Charles ED, Orloff MIM, Nishiuchi E, Marukian S, Rice CM, Dustin LB. Somatic hypermutations confer rheumatoid factor activity in hepatitis C virus-associated mixed cryoglobulinemia. Arthritis Rheum 2013;65:2430–2440.
[17] Comarmond C, Garrido M, Pol S, Desbois A-C, Costopoulos M, Le Garff-Tavernier M, et al. Direct-acting antiviral therapy restores immune tolerance to patients with hepatitis C virus-induced cryoglobulinemia vasculitis. Gastroenterology 2017;152, 2052–2062.e2.
[18] Lorin V, Mouquet H. Efficient generation of human IgA monoclonal antibodies. J Immunol Methods 2015;422:102–110.
[19] Wardemann H, Yurasov S, Schaefer A, Young JW, Meffre E, Nussenzweig MC. Predominant autoantibody production by early human B cell precursors. Science 2003;301:1374–1377.
[20] Tiller T, Meffre E, Yurasov S, Tsuiji M, Nussenzweig MC, Wardemann H. Efficient generation of monoclonal antibodies from single human B cells by single cell RT-PCR and expression vector cloning. J Immunol Methods 2008;329:112–124.
[21] Uduman M, Yaari G, Hershberg U, Stern JA, Shlomchik MJ, Kleinstein SH. Detecting selection in immunoglobulin sequences. Nucleic Acids Res 2011;39:W499–W504.
[22] Yaari G, Uduman M, Kleinstein SH. Quantifying selection in high-throughput Immunoglobulin sequencing data sets. Nucleic Acids Res 2012;40 e134.
[23] **Mouquet H**, **Scharf L**, Euler Z, Liu Y, Eden C, Scheid JF, et al. Complex-type N-glycan recognition by potent broadly neutralizing HIV antibodies. Proc Natl Acad Sci U S A 2012;109:E3268–E3277.
[24] Prigent J, Lorin V, Kök A, Hieu T, Bourgeau S, Mouquet H. Scarcity of autoreactive human blood IgA (+) memory B cells. Eur J Immunol 2016;46:2340–2351.
[25] Mouquet H, Farci S, Joly P, Maillère B, Leblond J, Drouot L, et al. A truncated alternative spliced isoform of human desmoglein 1 contains a specific T cell epitope binding to the pemphigus foliaceus-associated HLA class II DRbeta1*0102 molecule. J Immunol (Baltim Md 1950) 2006;177:6517–6526.
[26] Meffre E, Schaefer A, Wardemann H, Wilson P, Davis E, Nussenzweig MC. Surrogate light chain expressing human peripheral B cells produce self-reactive antibodies. J Exp Med 2004;199:145–150.
[27] Lau D, Lan LY-L, Andrews SF, Henry C, Rojas KT, Neu KE, et al. Low CD21 expression defines a population of recent germinal center graduates primed for plasma cell differentiation. Sci. Immunol. 2017;2, pii: eaai8153.
[28] Karnell JL, Kumar V, Wang J, Wang S, Voynova E, Ettinger R. Role of CD11c+ T-bet+ B cells in human health and disease. Cell Immunol 2017;321:40–45.

[29] Portugal S, Obeng-Adjei N, Moir S, Crompton PD, Pierce SK. Atypical memory B cells in human chronic infectious diseases: An interim report. Cell Immunol 2017;321:18–25.
[30] Liu F, Fan H, Ren D, Dong G, Hu E, Ji J, et al. TLR9-induced miR-155 and Ets-1 decrease expression of CD1d on B cells in SLE. Eur J Immunol 2015;45:1934–1945.
[31] Simchoni N, Cunningham-Rundles C. TLR7- and TLR9-responsive human B cells share phenotypic and genetic characteristics. J Immunol (Baltim Md 1950) 2015;194:3035–3044.
[32] Kong F, Zhang W, Feng B, Zhang H, Rao H, Wang J, et al. Abnormal CD4 + T helper (Th) 1 cells and activated memory B cells are associated with type III asymptomatic mixed cryoglobulinemia in HCV infection. Virol J 2015;12:100.
[33] Saadoun D, Rosenzwajg M, Joly F, Six A, Carrat F, Thibault V, et al. Regulatory T-cell responses to low-dose interleukin-2 in HCV-induced vasculitis. N Engl J Med 2011;365:2067–2077.
[34] Landau D-A, Rosenzwajg M, Saadoun D, Trébeden-Negre H, Klatzmann D, Cacoub P. Correlation of clinical and virologic responses to antiviral treatment and regulatory T cell evolution in patients with hepatitis C virus-induced mixed cryoglobulinemia vasculitis. Arthritis Rheum 2008;58:2897–2907.
[35] Elton TS, Selemon H, Elton SM, Parinandi NL. Regulation of the MIR155 host gene in physiological and pathological processes. Gene 2013;532:1–12.
[36] Sánchez-Zamora YI, Juarez-Avelar I, Vazquez-Mendoza A, Hiriart M, Rodriguez-Sosa M. Altered macrophage and dendritic cell response in Mif-/- mice reveals a role of Mif for inflammatory-Th1 response in type 1 diabetes. J. Diabetes Res 2016;2016:7053963.
[37] Shima H, Takatsu H, Fukuda S, Ohmae M, Hase K, Kubagawa H, et al. Identification of TOSO/FAIM3 as an Fc receptor for IgM. Int Immunol 2010;22:149–156.
[38] Sasaki M, Tojo A, Okochi Y, Miyawaki N, Kamimura D, Yamaguchi A, et al. Autoimmune disorder phenotypes in Hvcn1-deficient mice. Biochem J 2013;450:295–301.
[39] Hom G, Graham RR, Modrek B, Taylor KE, Ortmann W, Garnier S, et al. Association of systemic lupus erythematosus with C8orf13-BLK and ITGAM-ITGAX. N Engl J Med 2008;358:900–909.
[40] Gourh P, Agarwal SK, Martin E, Divecha D, Rueda B, Bunting H, et al. Association of the C8orf13-BLK region with systemic sclerosis in North-American and European populations. J Autoimmun 2010;34:155–162.
[41] Torres O, Palomino-Morales R, Vazquez-Rodriguez TR, Castañeda S, Morado IC, Miranda-Filloy JA, et al. Role of the C8orf13-BLK region in biopsy-proven giant cell arteritis. Hum Immunol 2010;71:525–529.
[42] De Re V, Sansonno D, Simula MP, Caggiari L, Gasparotto D, Fabris M, et al. HCV-NS3 and IgG-Fc crossreactive IgM in patients with type II mixed cryoglobulinemia and B-cell clonal proliferations. Leukemia 2006;20:1145–1154.
[43] Hu Y-W, Rocheleau L, Larke B, Chui L, Lee B, Ma M, et al. Immunoglobulin mimicry by hepatitis C virus envelope protein E2. Virology 2005;332:538–549.
[44] Ng PP, Kuo C-C, Wang S, Einav S, Arcaini L, Paulli M, et al. B-cell receptors expressed by lymphomas of hepatitis C virus (HCV)-infected patients rarely react with the viral proteins. Blood 2014;123:1512–1515.
[45] Moir S, Ho J, Malaspina A, Wang W, DiPoto AC, O'Shea MA, et al. Evidence for HIV-associated B cell exhaustion in a dysfunctional memory B cell compartment in HIV-infected viremic individuals. J Exp Med 2008;205:1797–1805.
[46] Kardava L, Moir S, Shah N, Wang W, Wilson R, Buckner CM, et al. Abnormal B cell memory subsets dominate HIV-specific responses in infected individuals. J Clin Invest 2014;124:3252–3262.
[47] Muellenbeck MF, Ueberheide B, Amulic B, Epp A, Fenyo D, Busse CE, et al. Atypical and classical memory B cells produce Plasmodium falciparum neutralizing antibodies. J Exp Med 2013;210:389–399.
[48] Nicholas MW, Dooley MA, Hogan SL, Anolik J, Looney J, Sanz I, et al. A novel subset of memory B cells is enriched in autoreactivity and correlates with adverse outcomes in SLE. Clin Immunol Orlando Fla 2008;126:189–201.
[49] Terrier B, Nagata S, Ise T, Rosenzwajg M, Pastan I, Klatzmann D, et al. CD21 (-/low) marginal zone B cells highly express Fc receptor-like 5 protein and are killed by anti-Fc receptor-like 5 immunotoxins in hepatitis C virus-associated mixed cryoglobulinemia vasculitis. Arthritis Rheumatol Hoboken NJ 2014;66:433–443.
[50] Chang L-Y, Li Y, Kaplan DE. Hepatitis C viraemia reversibly maintains subset of antigen-specific T-bet+ tissue-like memory B cells. J Viral Hepat 2017;24:389–396.
[51] Portugal S, Tipton CM, Sohn H, Kone Y, Wang J, Li S, et al. Malaria-associated atypical memory B cells exhibit markedly reduced B cell receptor signaling and effector function. eLife 2015;4.
[52] Kardava L, Moir S, Wang W, Ho J, Buckner CM, Posada JG, et al. Attenuation of HIV-associated human B cell exhaustion by siRNA downregulation of inhibitory receptors. J Clin Invest 2011;121:2614–2624.
[53] Wang Z, Wang Z, Wang J, Diao Y, Qian X, Zhu N. T-bet-expressing B cells are positively associated with Crohn's disease activity and support Th1 inflammation. DNA Cell Biol 2016;35:628–635.
[54] Rakhmanov M, Keller B, Gutenberger S, Foerster C, Hoenig M, Driessen G, et al. Circulating CD21low B cells in common variable immunodeficiency resemble tissue homing, innate-like B cells. Proc Natl Acad Sci U S A 2009;106:13451–13456.
[55] Claes N, Fraussen J, Vanheusden M, Hellings N, Stinissen P, Van Wijmeersch B, et al. Age-associated B cells with proinflammatory characteristics are expanded in a proportion of multiple sclerosis patients. J Immunol (Baltim Md 1950) 2016;197:4576–4583.
[56] Buchta CM, Bishop GA. Toll-like receptors and B cells: functions and mechanisms. Immunol Res 2014;59:12–22.
[57] Sindhava VJ, Oropallo MA, Moody K, Naradikian M, Higdon LE, Zhou L, et al. A TLR9-dependent checkpoint governs B cell responses to DNA-containing antigens. J Clin Invest 2017;127:1651–1663.
[58] Naradikian MS, Myles A, Beiting DP, Roberts KJ, Dawson L, Herati RS, et al. Cutting edge: IL-4, IL-21, and IFN-γ interact to govern T-bet and CD11c expression in TLR-activated B cells. J Immunol (Baltim Md 1950) 2019;197:1023–1028.
[59] Rivera-Correa J, Guthmiller JJ, Vijay R, Fernandez-Arias C, Pardo-Ruge MA, Gonzalez S, et al. Plasmodium DNA-mediated TLR9 activation of T-bet+ B cells contributes to autoimmune anaemia during malaria. Nat Commun 2017;8:1282.
[60] Leadbetter EA, Rifkin IR, Hohlbaum AM, Beaudette BC, Shlomchik MJ, Marshak-Rothstein A. Chromatin-IgG complexes activate B cells by dual engagement of IgM and Toll-like receptors. Nature 2002;416:603–607.
[61] Kortylewski M, Kujawski M, Wang T, Wei S, Zhang S, Pilon-Thomas S, et al. Inhibiting Stat3 signaling in the hematopoietic system elicits multicomponent antitumor immunity. Nat Med 2005;11:1314–1321.
[62] Oracki SA, Walker JA, Hibbs ML, Corcoran LM, Tarlinton DM. Plasma cell development and survival. Immunol Rev 2010;237:140–159.
[63] Saadoun D, Terrier B, Bannock J, Vazquez T, Massad C, Kang I, et al. Expansion of autoreactive unresponsive CD21-/low B cells in Sjögren's syndrome-associated lymphoproliferation. Arthritis Rheum 2013;65:1085–1096.
[64] Meffre E, Louie A, Bannock J, Kim LJY, Ho J, Frear CC, et al. Maturational characteristics of HIV-specific antibodies in viremic individuals. JCI Insight 2016;1.
[65] Bonagura VR, Agostino N, Børretzen M, Thompson KM, Natvig JB, Morrison SL. Mapping IgG epitopes bound by rheumatoid factors from immunized controls identifies disease-specific rheumatoid factors produced by patients with rheumatoid arthritis. J Immunol (Baltim Md 1950) 1998;160:2496–2505.
[66] Corper AL, Sohi MK, Bonagura VR, Steinitz M, Jefferis R, Feinstein A, et al. Structure of human IgM rheumatoid factor Fab bound to its autoantigen IgG Fc reveals a novel topology of antibody-antigen interaction. Nat Struct Biol 1997;4:374–381.
[67] Duquerroy S, Stura EA, Bressanelli S, Fabiane SM, Vaney MC, Beale D, et al. Crystal structure of a human autoimmune complex between IgM rheumatoid factor RF61 and IgG1 Fc reveals a novel epitope and evidence for affinity maturation. J Mol Biol 2007;368:1321–1331.
[68] Kong L, Giang E, Nieusma T, Kadam RU, Cogburn KE, Hua Y, et al. Hepatitis C virus E2 envelope glycoprotein core structure. Science 2013;342:1090–1094.
[69] Chan CH, Hadlock KG, Foung SK, Levy S. V (H)1–69 gene is preferentially used by hepatitis C virus-associated B cell lymphomas and by normal B cells responding to the E2 viral antigen. Blood 2001;97:1023–1026.
[70] Quinn ER, Chan CH, Hadlock KG, Foung SK, Flint M, Levy S. The B-cell receptor of a hepatitis C virus (HCV)-associated non-Hodgkin lymphoma binds the viral E2 envelope protein, implicating HCV in lymphomagenesis. Blood 2001;98:3745–3749.
[71] Deisenhofer J. Crystallographic refinement and atomic models of a human Fc fragment and its complex with fragment B of protein A from Staphylococcus aureus at 2.9- and 2.8-A resolution. Biochemistry 1981;20:2361–2370.